IEEE Access
Multidisciplinary | Rapid Review | Open Access Journal

SPECIAL SECTION ON ADVANCED MODELING AND CONTROL OF COMPLEX MECHATRONIC SYSTEMS WITH NONLINEARITY AND UNCERTAINTY

Received March 27, 2018, accepted May 20, 2018, date of publication May 28, 2018, date of current version June 19, 2018.

Digital Object Identifier 10.1109/ACCESS.2018.2841514

Discrete-Time Adaptive Control Design for Ionic Polymer-Metal Composite Actuators

XINKAI CHEN, (Senior Member, IEEE)
Department of Electronic Information Systems, Shibaura Institute of Technology, Saitama 337-8570, Japan
e-mail: chen@sic.shibaura-it.ac.jp

This work was supported by the Grants-in-Aid for Scientific Research of the Japan Society for the Promotion of Science under Grants C-15K06152, C-18K04212, and 14032011-000073.

ABSTRACT Discrete-time adaptive control for ionic polymer-metal composite (IPMC) actuator is studied in this paper. First, a new mathematical model in discrete-time domain is proposed for IPMC actuator. Then, based on the obtained model, a discrete adaptive control law is synthesized for IPMC actuators. The proposed discrete adaptive controller can guarantee the global stability of the closed-loop system, and the position tracking error of the IPMC actuator can be controlled by the design parameters. Finally, the proposed model and control law are verified by IPMC actuator experiments.

INDEX TERMS IPMC, discrete-time adaptive control, hysteresis, Prandtl-Ishlinskii model.

I. INTRODUCTION

Ionic polymer-metal composite (IPMC) is an important electroactive polymer which has promising applications in bio-mechatronics field due to its actuation capability [2], [15], [17]. A typical IPMC actuator is composed of a pair of noble metal-based electrodes and a thin membrane which has the function of ion exchange, where the electrodes are plated chemically on both faces of the membrane. When a voltage is applied, hydrated cations and water molecules move within the IPMC, and this will lead to bending motion, and thus the actuation effect of IPMC. Fig. 1 shows the IPMC actuation mechanism under an applied voltage. IPMCs receives much attention in biomedical device and biomimetic robot fields recently [4], [7], [16] because of its biocompatibility, resilience, softness, and the large force and large deformation generation capability under a low voltage. Recently, IPMC are even expected to be applied in micro/nano manipulation areas. However, the major disadvantage of the IPMCs is the existence of the hysteresis nonlinearity between the input voltage and the output displacement. The measured relation is shown in Fig. 2, where an IPMC actuator of Environmental Robots Inc. is used, and the applied voltage is expressed as $\frac{2\sin(0.1\pi k)}{1+\frac{k}{70}}$ [V] for $k = 1, 2, \cdots, 120$ and the sampling period is 0.03 second. Since the hysteresis is highly nonlinear and has nonmemoryless characteristics, it will inevitably cause positioning errors which will severely affect the precision and actuation speed of the IPMCs. Modeling of hysteresis and elimination of the effects of hysteresis have received extensive attention recently due to the development of smart materials in which hysteresis usually exists, where traditional control methods in [1] and [9] are insufficient and ineffective.

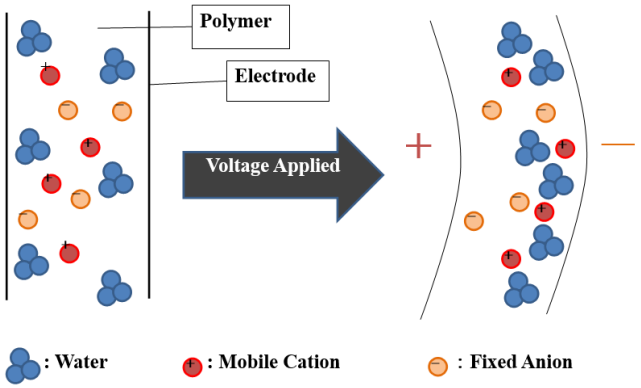

FIGURE 1. Actuation mechanism of IPMC actuators.

About the modeling and control design for the systems with hysteresis, the mathematical characterization of the nonlinearities stands at the very important position [3], [7], and it is still a well-known open problem. Until now, many famous hysteresis models have been proposed in the literature. However, a hysteresis model suitable for controller design is highly desired to describe the hysteretic nonlinearities for its possible application in synthesizing control laws. In this

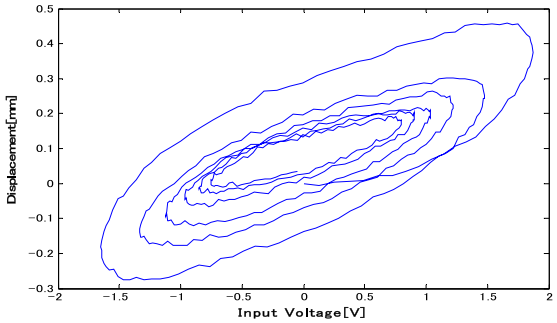

FIGURE 2. Measured hysteretic relation between the input voltage and the output displacement.

paper, the hysteresis models which are based on operators will be employed. The operator-based hysteresis models consists of weighted aggregate effects of a group of elementary hysteresis operators with similar mathematical structures. Famous operator-based hysteresis models are Krasnosel'skii-Pokrovskii (KP) model [3], [11], Prandtl-Ishlinskii (PI) model [5], [10], Preisach model [11], [14], [21], etc. KP model and Preisach model are parameterized by two thresholds, whereas the PI model is relatively simple and is parameterized by one threshold.

In this paper, a mathematical model of IPMC actuator oriented in control design will be firstly constructed. Then, the next work will be finding the appropriate control methods to apply to the obtained models to minimize the effects of hysteresis which is usually unknown in practice. However, the results on this topic are very rare in [5] and [18]–[20]. The most popular solution in dealing with hysteresis is constructing its explicit inverse operator to cancel it in [10] and [20], which is firstly proposed in [20]. An alternative approach is to construct an implicit inverse of the hysteresis [5], [6]. This approach is proposed in order to solve the problem existing in the explicit inverse method in which the closed-loop stability cannot be analyzed and the tracking error cannot be prescribed. The implicit inverse is derived online by finding an appropriate value, which can be obtained by finite steps of operation, at each instant to perform a prescribed control index.

In this paper, firstly, a phenomenological model for IPMC actuator is proposed in discrete-time domain. The model is a linear discrete-time system preceded by a PI hysteretic operator. A discrete adaptive control law is synthesized based on the proposed model. Only the parameters in the control law expression are needed to be adaptively estimated. The proposed discrete-time adaptive control guarantees the global stability of the closed-loop system, and the tracking error of the end position of the IPMC actuator can be controlled by tuning the design parameters. Experimental results for different desired position signals are presented to show the effectiveness of the proposed model and control.

In the following of this paper, Section II states the problem, where the mathematical model in discrete-time domain of the IPMC actuator is presented. In Section III, the discrete-time adaptive control and the analysis of the closed-loop system are addressed. In Section IV, the proposed control law is illustrated by experiments. Section V gives the conclusion of the paper.

II. PROBLEM STATEMENT

A. PRANDTL-ISHLINSKII (PI) HYSTERESIS OPERATOR

By observing the behavior of the genuine input-output relation given in Fig. 2, it can be seen that a strong hysteretic nonlinearity exists. In order to characterize this nonlinearity, Prandtl-Ishlinskii (PI) hysteresis operator will be introduced.

The basic element of PI hysteresis is the so-called "play operator." For a given piece-wise monotonic function $u(k)$ and a value $\omega \in R$, a new function $p_\alpha : R \times R \to R$ is defined as

$$p_\alpha(u, \omega) = \max(u - \alpha, \min(u + \alpha, \omega)), \tag{1}$$

where α is the threshold satisfying $\alpha \geq 0$. Suppose the initial value of the play operator is $v_{-1} \in R$ and $u(k)$ is monotone for $k_i \leq k \leq k_{i+1}$, the play operator $P_\alpha[\cdot; v_{-1}](k)$ can be defined as

$$P_\alpha[u; v_{-1}](0) = p_\alpha(u(0), v_{-1}), \tag{2}$$

$$P_\alpha[u; v_{-1}](k) = p_\alpha(u(k), P_\alpha[u; v_{-1}](k_i)), \tag{3}$$

for any k satisfying $k_i \leq k \leq k_{i+1}$ Thus, the function $P_\alpha[u; v_{-1}](k)$ is mainly determined by $u(k)$ and α.

Now, let us denote the hysteresis relation between $u(k)$ and $v(k)$ as $v(k) = H[u](k)$. The details of this relation is a simple version of PI model [3], [14],

$$v(k) = \sum_{i=1}^{r} \gamma_i P_{\alpha_i}[u; v_{-1}](k), \tag{4}$$

where r is a positive integer denoting the number of play operators needed in the PI model; γ_i are the corresponding weights of the play operators satisfying $\gamma_1 > 0$ and $\gamma_i \geq 0$ for $i \geq 2$; the thresholds α_i meet $\alpha_1 = 0$ and $\alpha_i < \alpha_j$ if $i < j$.

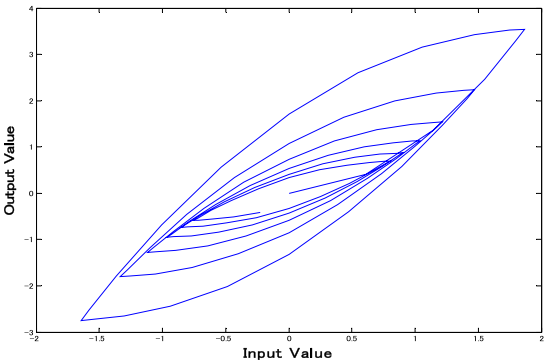

FIGURE 3. Hysteresis curve generated by (4).

Fig. 3 shows the generated curve between $u(k)$ and $v(k)$ with $r = 10$, $\gamma_i = e^{-0.1(0.2i-1)^2}$, $\alpha_i = 0.2i$,

$u(k) = \frac{2\sin(0.1\pi k)}{1+\frac{k}{70}}$ for $k = 1, 2, \cdots, 120$, where a hysteresis relation can be observed.

Lemma 1: Consider the operator $H[\cdot]$ given in (4), there exist positive integer ϖ, density parameters β_i with $\beta_1 > 0$, $\beta_i \leq 0$ for $i \geq 2$ and thresholds λ_i satisfying $\lambda_1 = 0$ and $\lambda_i < \lambda_j$ if $i < j$ such that

$$u(k) = \sum_{i=1}^{\varpi} \beta_i P_{\lambda_i}[v;\ 0](k). \tag{5}$$

Proof: See [14].

For compactness, denote $P_{\alpha_i}[u, v_{-1}](k)$ by $P_{\alpha_i}[u](k)$ in the following of this paper.

Lemma 2: For the relation of $u(k)$ and $v(k)$, there exist constants $K_1 > 0$ and $K_2 > 0$ such that

$$|u(k)| \leq K_1 \max_{1\leq\tau\leq k} |v(\tau)| \tag{6}$$

and

$$|v(k)| \leq K_2 \max_{1\leq\tau\leq k} |u(\tau)|. \tag{7}$$

Proof: For any signal $\psi(k)$, it is obvious that $|P_\alpha[\psi](k)| \leq \max_{1\leq\tau\leq k} |\psi(\tau)|$. From this fact and Lemma 1, relations (6) and (7) are obvious.

B. MODEL FORMULATION AND CONTROL PURPOSE

By observing Fig. 2 and Fig. 3 and comparing them, it is obvious that the PI model cannot satisfactorily characterize the hysteretic behavior in the input-output relation of the IPMC actuator, particularly at the time instants when the input signal changes its monotonic properties. Now, in order to smoothen the sharpness at these instants, a filter

$$G(q^{-1}) = \frac{q^{-d}P(q^{-1})}{T(q^{-1})} \tag{8}$$

with

$$T(q^{-1}) = 1 + t_1 q^{-1} + \cdots + t_n q^{-n} \tag{9}$$
$$P(q^{-1}) = 1 + p_1 q^{-1} + \cdots + p_m q^{-m} \tag{10}$$

is attached to the output side of the PI operator to characterize the dynamics of the IPMC actuators, where q^{-1} is the time delay defined as

$$q^{-1}v(k) = v(k-1) \tag{11}$$

m, n and d are positive integers with $m \leq n$; t_i and p_j are constants for $i = 1, \cdots, n$ and $j = 1, \cdots, m$; $P(q^{-1})$ and $T(q^{-1})$ are coprime Schur polynomials. Thus, the model of the IPMC actuator is given in Fig. 4.

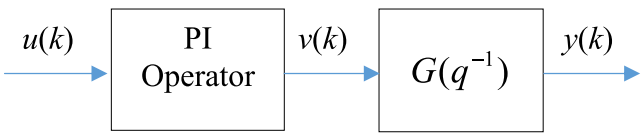

FIGURE 4. Model of IPMC actuator.

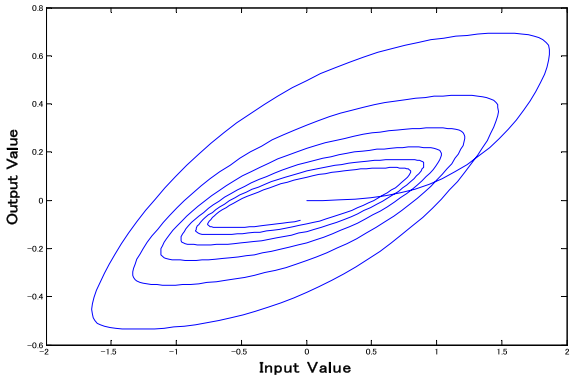

FIGURE 5. The generated relation of $u(k)$ and $y(k)$.

Figure 5 shows the generated relation of $u(k)$ and $y(k)$ with $G(q^{-1}) = \frac{q^{-2}(1+0.1q^{-1})}{1-1.5q^{-1}+0.75q^{-2}-0.125q^{-3}}$ where the PI operator used in generating Fig. 3 is employed. By comparing Fig. 2 and Fig. 5, it is obvious that the behaviors of the input-output relations are very similar. Thus, it can be argued that the model given in Fig. 4 has the ability of describing the input-output relation of IPMC actuators.

This paper aims to urge the displacement $y(k)$ to follow a desired signal $y_d(k)$ for the IPMC actuators.

III. ADAPTIVE CONTROL AND ANALYSIS

The discrete adaptive control law for IPMC actuators will be designed by using the model given in Fig. 4.

A. SOME PRELIMINARIES

First of all, for the Schur polynomial described by

$$C(q^{-1}) = 1 + c_1 q^{-1} + \cdots + c_n q^{-n} \tag{12}$$

define a new signal

$$s(k) = C(q^{-1})\left(y(k) - y_d(k)\right). \tag{13}$$

It can be seen that $\lim_{k\to\infty} s(k) = 0$ implies $\lim_{k\to\infty} (y(k) - y_d(k)) = 0$.

From the theory in [1] and [9], there exist unique polynomials $B(q^{-1})$ and $F(q^{-1})$ in the form

$$B(q^{-1}) = 1 + b_1 q^{-1} + \cdots + b_{d-1} q^{-d+1} \tag{14}$$
$$F(q^{-1}) = f_0 + f_1 q^{-1} + \cdots + f_{n-1} q^{-n+1} \tag{15}$$

satisfying the following polynomial equation

$$C(q^{-1}) = T(q^{-1})B(q^{-1}) + q^{-d}F(q^{-1}). \tag{16}$$

By acting on $y(k)$ of the both sides of Equation (16) and using Equation (8) and Fig. 4, it yields

$$C(q^{-1})y(k+d) = H(q^{-1})v(k) + F(q^{-1})y(k), \tag{17}$$

where $H(q^{-1})$ is defined as

$$\begin{aligned} H(q^{-1}) &= B(q^{-1})P(q^{-1}) \\ &= h_0 + h_1 q^{-1} + \cdots + h_{m+d-1} q^{-m-d+1} \end{aligned} \tag{18}$$

and $v(k)$ is the imaginary signal defined in Fig. 4.

Replacing $v(k)$ with the PI model (4) yields

$$\begin{aligned} &C(q^{-1})y(k+d) \\ &= F(q^{-1})y(k) + \sum_{i=1}^{r} h_0\gamma_i P_{\alpha_i}[u](k) + \sum_{i=1}^{r} h_1\gamma_i P_{\alpha_i}[u](k-1) \\ &\quad + \cdots + \sum_{i=1}^{r} h_{m+d-1}\gamma_i P_{\alpha_i}[u](k-m-d+1) \\ &\triangleq \varphi^T(k)\theta \end{aligned} \tag{19}$$

with

$$\begin{aligned} \varphi(k) = \big[&P_{\alpha_1}[u](k), \cdots, P_{\alpha_r}[u](k), \cdots, \\ &P_{\alpha_1}[u](k-m-d+1), \cdots, P_{\alpha_r}[u](k-m-d+1) \\ &y(k), \cdots, y(k-n+1)\big]^T \end{aligned} \tag{20}$$

and

$$\begin{aligned} \theta = [&h_0\gamma_1, \cdots, h_0\gamma_r, \cdots, h_{m+d-1}\gamma_1, \cdots, h_{m+d-1}\gamma_r, \\ &f_0, \cdots, f_{n-1}]^T. \end{aligned} \tag{21}$$

When all the parameters are available, it can be seen that, if the input $u(k)$ satisfies

$$\begin{aligned} &\sum_{i=1}^{r} h_0\gamma_i P_{\alpha_i}[u](k) \\ &\quad = C(q^{-1})y(k+d) - F(q^{-1})y(k) \\ &\qquad + \rho \cdot s(k) - \sum_{i=1}^{r} h_1\gamma_i P_{\alpha_i}[u](k-1) \\ &\qquad - \cdots - \sum_{i=1}^{r} h_{m+d-1}\gamma_i P_{\alpha_i}[u](k-m-d+1) \end{aligned} \tag{22}$$

where ρ is a parameter with $0 < \rho < 1$, then the output tracking can be realized asymptotically. The introduction of $\rho \cdot s(k)$ in (22) is to tune the response performance of the closed-loop system.

B. ADAPTIVE ALGORITHM

In this paper, since the mathematical model of the IPMC is built phenomenologically, all the parameters in θ are unknown. Let

$$\hat{\theta}(k) = \left[\hat{\theta}_1(k), \cdots, \hat{\theta}_{r(m+d)+n}(k)\right]^T \tag{23}$$

denote the adaptive update value of θ at instant k, where $\hat{\theta}_i(k)$ is the corresponding estimate of the i-th element in θ.

From (19), it can be seen that, by replacing θ with $\hat{\theta}(k-1)$, $\varphi^T(k-d)\hat{\theta}(k-1)$ can be thought of the estimate of $C(q^{-1})y(k)$. Thus, the estimation error can be defined as

$$e(k) = C(q^{-1})y(k) - \varphi^T(k-d)\hat{\theta}(k-1) \tag{24}$$

From (19) and (24), the defined error $e(k)$ also has the form

$$e(k) = \varphi^T(k-d)\left(\theta - \hat{\theta}(k-1)\right) \tag{25}$$

The online estimation law of $\hat{\theta}(k)$ is constructed by the adaptation algorithms with constraints [9]

$$\hat{\theta}'(k) = \hat{\theta}(k) + \sigma \frac{e(k)\varphi(k-d)}{1+\varphi^T(k-d)\varphi(k-d)}, \tag{26}$$

$$\hat{\theta}_i(k) = \left|\hat{\theta}'_i(k)\right| \quad \text{for } i = 1, \cdots, r, \tag{27}$$

$$\hat{\theta}_j(k) = \hat{\theta}'_j(k) \quad \text{for } j = r+1, \cdots, r(m+d)+n, \tag{28}$$

where σ is the adaptation gain with $0 < \sigma < 2$. The initial values $\hat{\theta}_i(0)$ should satisfy $\hat{\theta}_i(0) > 0$ for $i = 1, \cdots, r$ and $\hat{\theta}_j(0) \geq 0$ for $j = r+1, \cdots, r(m+d)+n$.

Lemma 3: For the algorithm defined in (26)-(28), it yields

(P1) $\hat{\theta}(k)$ is uniformly bounded;

(P2) $\sum_{k=1}^{\infty} \frac{e(k)\varphi(k-d)}{1+\varphi^T(k-d)\varphi(k-d)} < \infty$;

(P3) $\lim_{k\to\infty} \frac{e(k)\varphi(k-d)}{1+\varphi^T(k-d)\varphi(k-d)} = 0$;

(P4) $\sum_{k=\upsilon}^{\infty} \left\|\hat{\theta}(k) - \hat{\theta}(k-\upsilon)\right\|_2^2 < \infty$ for arbitrary finite positive integer υ, where the norm $\|\zeta\|_2$ of a vector ζ is defined as

$$\|\zeta\|_2 = \left(\zeta^T\zeta\right)^{\frac{1}{2}}.$$

Proof: See [9] (Lemma 3.3.2).

C. ADAPTIVE CONTROL DESIGN

For simplicity, by observing (22), let us define a new signal

$$\begin{aligned} V(k) = &C(q^{-1})y(k+d) - \sum_{i=0}^{n-1} \hat{\theta}_{r(m+d)+i+1}(k)y(k-i) \\ &+ \rho \cdot s(k) - \sum_{i=1}^{r} \hat{\theta}_{r+i}(k)P_{\alpha_i}[u](k-1) \\ &- \cdots - \sum_{i=1}^{r} \hat{\theta}_{r(m+d-1)+i}(k)P_{\alpha_i}[u](k-m-d+1) \end{aligned} \tag{29}$$

It is clear that $V(k)$ is available at instant k.

Now, let us derive the signal $U^*(k)$ satisfying

$$\sum_{i=1}^{r} \hat{\theta}_i(k)P_{\alpha_i}[U^*](k) = V(k) \tag{30}$$

Remark 1: The introduction of (30) is motivated by (22). It can be expected that, if the input $u(k)$ is chosen as $U^*(k)$ which satisfies Equation (30), then $s(k)$ will converge to zero under the condition that $e(k)$ approaches to zero.

As a matter of fact, finding a signal $U^*(k)$ satisfying (30) is almost impossible in practice since $P_{\alpha_i}[\cdot]$ is very complicated nonlinear function. In this paper, for a prescribed admissible error ε, the signal $U^*(k)$ satisfying

$$\left|\sum_{i=1}^{r} \hat{\theta}_i(k)P_{\alpha_i}[U^*](k) - V(k)\right| \leq \varepsilon \tag{31}$$

will be searched for.

Without loss of generality, assume $V(k)$ is monotonically increasing with $k_j < k \le k_{j+1}$. Suppose $u_{\min}$ and $u_{\max}$ are the possible lower and higher input voltage to the IPMC actuator and define $\overline{V}(k)$ and $\underline{V}(k)$ as

$$\overline{V}(k) = \sum_{i=1}^{r} \hat{\theta}_i(k) P_{\alpha_i}[u_{\max}](k), \tag{32}$$

$$\underline{V}(k) = \sum_{i=1}^{r} \hat{\theta}_i(k) P_{\alpha_i}[u_{\min}](k). \tag{33}$$

Thus, it yields

$$\overline{V}(k) \le \sum_{i=1}^{r} \hat{\theta}_i(k) P_{\alpha_i}[u](k) \le \underline{V}(k) \tag{34}$$

for any $u_{\min} \le u(k) \le u_{\max}$.

If $V(k) > \overline{V}(k)$, let $U^*(k) = u_{\max}$;

If $V(k) < \underline{V}(k)$, let $U^*(k) = u_{\min}$;

If $\overline{V}(k) \le V(k) \le \underline{V}(k)$, the value of $U^*(k)$ will be derived with the next algorithm, where Δ is a small positive constant.

Step 1: $U^{(0)}(k) := U^*(k-1)$, $l := 0$.

Step 2: $x^{(l)}(k) := \sum_{i=1}^{r} \hat{\theta}_i(k) P_{\alpha_i}[U^{(l)}](k)$.

If $\left|x^{(l)}(k) - V(k)\right| \le \varepsilon$, go to Step 4;

Else if $x^{(l)}(k) < V(k) - \varepsilon$, let $U^{(l+1)}(k) := U^{(l)}(k) + \Delta$ and $l := l + 1$, then go to Step 2.

Else, let $\underline{U}^{(l)}(k) := U^{(l-1)}(k)$ and $\overline{U}^{(l)}(k) := U^{(l)}(k)$, then go to Step 3.

Step 3:

$$\underline{x}^{(l)}(k) := \sum_{i=1}^{r} \hat{\theta}_i(k) P_{\alpha_i}[\underline{U}^{(l)}](k),$$

$$\bar{x}^{(l)}(k) := \sum_{i=1}^{r} \hat{\theta}_i(k) P_{\alpha_i}[\overline{U}^{(l)}](k),$$

$$U^{(l+1)}(k) := \underline{U}^{(l)} + \Delta \frac{V(k) - \underline{x}^{(l)}(k)}{\bar{x}^{(l)}(k) - \underline{x}^{(l)}(k)}.$$

Let $l := l + 1$ and $x^{(l)}(k) := \sum_{i=1}^{r} \hat{\theta}_i(k) P_{\alpha_i}[U^{(l)}](k)$.

If $\left|x^{(l)}(k) - V(k)\right| \le \varepsilon$, go to Step 4;

Else if $x^{(l)}(k) < V(k) - \varepsilon$, let $\underline{U}^{(l)}(k) := U^{(l)}(k)$ and $\overline{U}^{(l)}(k) := \overline{U}^{(l-1)}(k)$, then return to Step 3;

Else, let $\underline{U}^{(l)}(k) := \underline{U}^{(l-1)}(k)$ and $\overline{U}^{(l)}(k) := U^{(l)}(k)$, then return to Step 3.

Step 4: $U^*(k) := U^{(l)}(k)$ and stop.

Remark 2: It can be seen that finite times of operations will result in the finding of $U^*(k)$ satisfying (31), i.e. the index l is finite when the searching operation is finished.

Remark 3: If $V(k)$ is monotonically decreasing on $k_j < k \le k_{j+1}$, the algorithm of searching for $U^*(k)$ can be similarly formulated.

Upon the above preparations, the input voltage is chosen as

$$u(k) = U^*(k). \tag{35}$$

D. ANALYSIS OF THE CLOSED-LOOP SYSTEM

In this subsection, suppose $\overline{V}(k) \le V(k) \le \underline{V}(k)$.

By observing (29), (31) and (35), it gives

$$\varphi^T(k)\hat{\theta}(k) = C(z^{-1}) y_d(k+d) + \rho s(k) + \eta(k) \tag{36}$$

with

$$\eta(k) = \sum_{i=1}^{r} \hat{\theta}_i(k) P_{\alpha_i}[U^*](k) - V(k) \tag{37}$$

satisfying

$$|\eta(k)| \le \varepsilon. \tag{38}$$

Combining (19) and (36) yields

$$\varphi^T(k)\theta = C(q^{-1}) y_d(k+d) + \rho s(k) + \eta(k) + e(k+d) + \xi(k), \tag{39}$$

i.e.

$$F(q^{-1})y(k) + H(q^{-1})v(k) = C(q^{-1}) y_d(k+d) + \rho s(k) + \eta(k) + e(k+d) + \xi(k) \tag{40}$$

with

$$\xi(k) = \varphi^T(k)\left(\hat{\theta}(k+d-1) - \hat{\theta}(k)\right). \tag{41}$$

By (17) and (40), the dynamics of $s(k)$ defined in (13) gives

$$s(k+d) = \rho s(k) + \eta(k) + e(k+d) + \xi(k). \tag{42}$$

By integrating (8), (40) and (42) together, the global system can be expressed

$$\begin{bmatrix} T(q^{-1}) & -q^{-d}P(q^{-1}) & 0 \\ F(q^{-1}) & H(q^{-1}) & -\rho \\ 0 & 0 & 1-\rho q^{-d} \end{bmatrix} \begin{bmatrix} y(k) \\ v(k) \\ s(k) \end{bmatrix} = \begin{bmatrix} 0 \\ 1 \\ q^{-d} \end{bmatrix} (e(k+d) + \eta(k) + \xi(k)) + \begin{bmatrix} 0 \\ 1 \\ 0 \end{bmatrix} \times C(q^{-1}) y_d(k+d). \tag{43}$$

Theorem 1: For the IPMC actuator modeled in Fig.4 controlled by the input (35), all the signals in the closed-loop are uniformly bounded, $\lim_{k\to\infty} e(k) = 0$, and

$$\lim_{k\to\infty} \sup |y(k) - y_d(k)| = \mu\varepsilon, \tag{44}$$

where μ is a positive constant depending on ρ and $C(q^{-1})$.

Proof: For system (43),

$$\det \begin{bmatrix} T(q^{-1}) & -q^{-d}P(q^{-1}) & 0 \\ F(q^{-1}) & H(q^{-1}) & -\rho \\ 0 & 0 & 1-\rho q^{-d} \end{bmatrix} = C(q^{-1})P(q^{-1})\left(1-\rho q^{-d}\right)$$

is a Schur polynomial. Thus, by observing the uniform boundedness of $y_d(k)$ and $\eta(k)$, there exist constants $C_1 > 0$ and $C_2 > 0$ such that

$$\|\phi(k)\|_2 \le C_1 + C_2 \left\{ \max_{1\le\tau\le k} |e(\tau+d)| + \max_{1\le\tau\le k} |\xi(\tau)| \right\}, \tag{45}$$

with

$$\phi(k) = [y(k), \cdots, y(k-n+1), v(k), \cdots, v(k-m-d+1), s(k)]^T. \tag{46}$$

Since $|P_\alpha[\psi](k)| \le \max_{1\le\tau\le k} |\psi(\tau)|$ for any signal $\psi(k)$, from (20), it can be easily seen that

$$\|\varphi(k)\|_2^2 \le r(m+d) \max_{1\le\tau\le k} u^2(\tau) + y^2(k) + \cdots + y^2(k-n+1). \tag{47}$$

By Lemma 3, there exist constants $C_3 > 0$ and $C_4 > 0$ such that

$$\begin{aligned}\|\varphi(k)\|_2^2 &\le C_3 \max_{1\le\tau\le k} v^2(\tau) + y^2(k) + \cdots + y^2(k-n+1) \\ &\le C_4 \max_{1\le\tau\le k} \Big(y^2(\tau) + \cdots + y^2(\tau-n+1) + v^2(\tau) \\ &\quad + \cdots + v^2(\tau-m-d+1) \Big) \\ &\le C_4 \max_{1\le\tau\le k} \|\phi(\tau)\|^2. \end{aligned} \tag{48}$$

From (45) and (48), there exist constants $C_5 > 0$ and $C_6 > 0$ such that

$$\|\varphi(k)\|_2 \le C_5 + C_6 \left\{ \max_{1\le\tau\le k} |e(\tau+d)| + \max_{1\le\tau\le k} |\xi(\tau)| \right\} \tag{49}$$

By (41) and Lemma 3, there is a constant $C_7 > 0$ such that

$$C_6 \max_{1\le\tau\le k} |\xi(\tau)| \le C_7 + \frac{1}{2} \max_{1\le\tau\le k} \|\varphi(k)\|_2. \tag{50}$$

Then, from (49) and (50), there exist constants $C_8 > 0$ and $C_9 > 0$ such that

$$\|\varphi(k-d)\|_2 \le C_8 + C_9 \max_{1\le\tau\le k} |e(\tau)|. \tag{51}$$

So, [9, Lemma 6.2.1] can be applied to P3 of Lemma 3, and it yields $\lim_{k\to\infty} e(k) = 0$. Thus, relation (51) implies that all signals in the closed-loop are uniformly bounded. Further, by recalling the expression of $\xi(k)$ in (41) and Lemma 3, it gives $\lim_{k\to\infty} \xi(k) = 0$. Then, by (38) and (42), the following relation can be easily derived.

$$\lim_{k\to\infty} \sup |s(k)| \le \frac{1}{1-\rho}\varepsilon \tag{52}$$

Therefore, relation (44) is valid by using the definition of $s(k)$.

Remark 4: (44) implies that output tracking error is dominated by the roots of $C(q^{-1})$ and the parameters ε and ρ.

Remark 5: The introduction of ρ $(0 < \rho < 1)$ in (29) is to tune the system performance and to regulate the magnitude of the input. The value of ρ needs to be enlarged if the magnitude of the input is too big [6].

IV. EXPERIMENTAL RESULTS

Fig. 6 shows the experimental setup of the system, where the used IPMC actuator is made by Environmental Robots Inc. In this paper, the sampling rate is set as 0.03 second.

FIGURE 6. Experimental setup for IPMC actuator.

First, the experiment is conducted for $y_{d1}(k) = 0.2mm$. Experiments for various choices of d, n, and m have been conducted. The best results have been obtained when d, n, and m are chosen as d=2, n=3 and m=1, and the polynomial $C(q^{-1})$ is set to

$$C(q^{-1}) = 1 - 1.5q^{-1} + 0.75q^{-2} - 0.125q^{-3}.$$

The value of r in (4) is chosen as $r = 10$. The initial values $\hat{\theta}_i(0)$ of the parameter adaption algorithm are chosen as

$$\hat{\theta}_{10(j-1)+i}(0) = 0.2e^{-0.1(0.2i-1)^2}$$

for $i = 1, \cdots, 10$ and $j = 1, 2, 3$;

$$\hat{\theta}_l(0) = 0.1$$

for $l = 31, 32, 33$.

The design parameters in the control are chosen as that shown in Table 1.

TABLE 1. Design parameters.

ρ	0.1
σ	0.2
ε	10^{-4}
Δ	0.1

The control input for $y_{d1}(k)$ is shown in Fig. 7, and the tracking error is given in Fig. 8 where the steady state tracking error is within the range $\pm 0.01mm$.

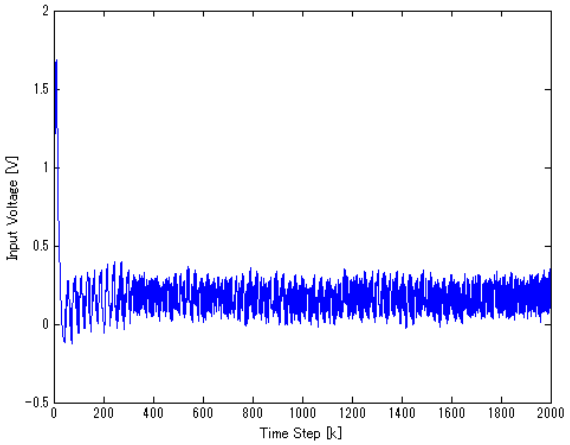

FIGURE 7. Control input for $y_{d1}(k)$.

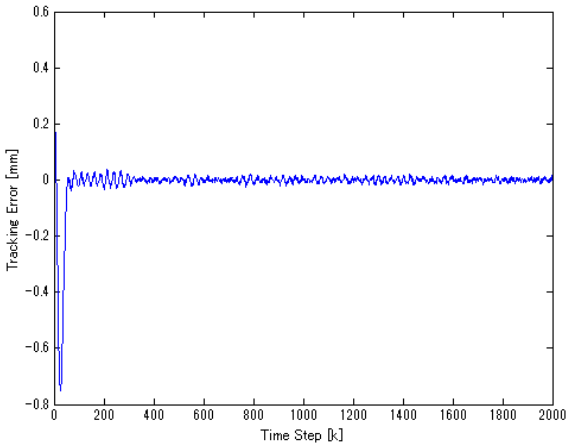

FIGURE 8. Tracking error for $y_{d1}(k)$.

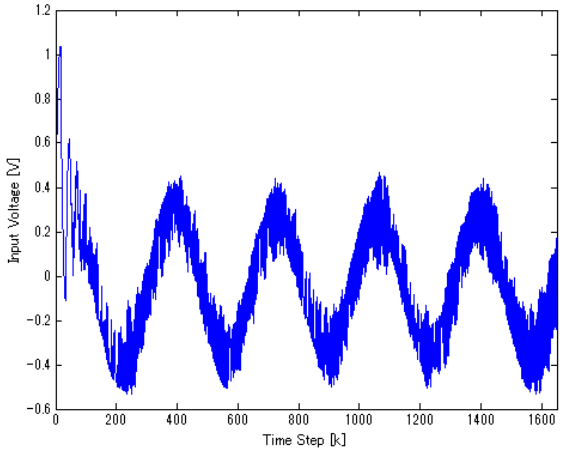

FIGURE 9. Control input for $y_{d2}(k)$ with $f = 0.1$.

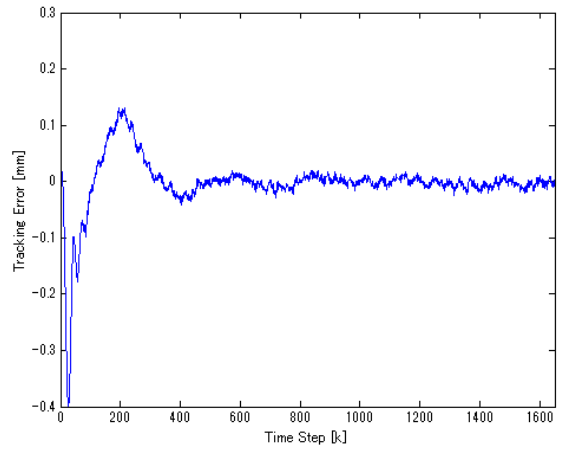

FIGURE 10. Tracking error for $y_{d2}(k)$ with $f = 0.1$.

To test the robustness of the proposed control algorithm and the control parameters, the same controller is applied to desired output signals

$$y_{d2}(k) = 0.2 \sin\left(2\pi f(30 \times 10^{-3})k\right) [mm]$$

where f is the frequency. The control input for $y_{d2}(k)$ with $f = 0.1$ is given in Fig. 9. The tracking error for this desired output is illustrated in Fig. 10, where the steady state error remains in the range $\pm 0.015mm$.

Fig. 11 shows the control input for $y_{d2}(k)$ with $f = 0.3$. The tracking error for this desired output is given in Fig. 12, where the steady state error remains in the range $\pm 0.02mm$.

Fig. 13 shows the control input for $y_{d2}(k)$ with $f = 0.6$. The tracking error for this desired output is illustrated in Fig. 14, where steady state error remains in the range $\pm 0.04mm$.

The experimental results show that the tracking error will become larger and larger when the frequency of the desired output signal becomes higher and higher. However, when the frequency is near 1, the tracking error becomes 100% of the output which is no longer acceptable in practice. One main reason is that the movement of the cations and water molecules inside IPMC materials cannot be performed at a frequency higher than 1.

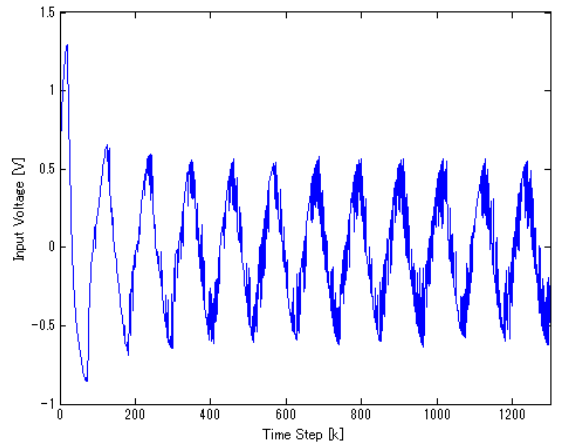

FIGURE 11. Control input for $y_{d2}(k)$ with $f = 0.3$.

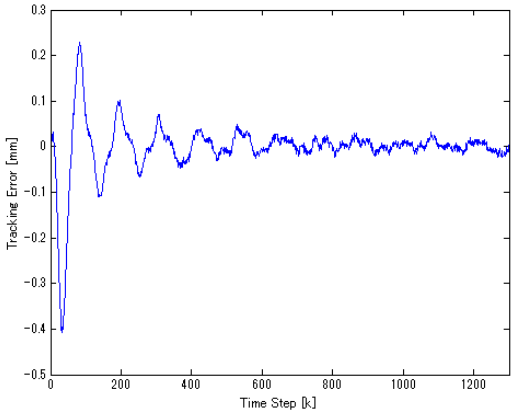

FIGURE 12. Tracking error for $y_{d2}(k)$ with $f = 0.3$.

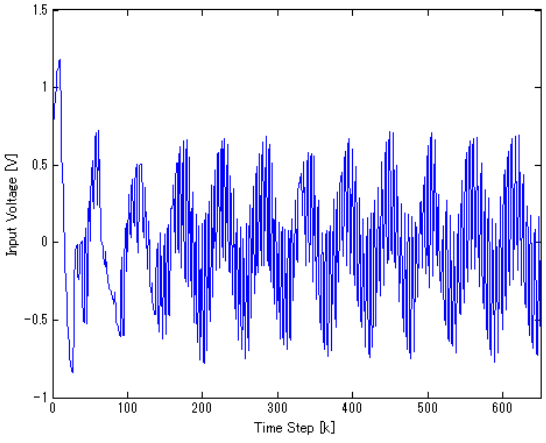

FIGURE 13. Control input for $y_{d2}(k)$ with $f = 0.6$.

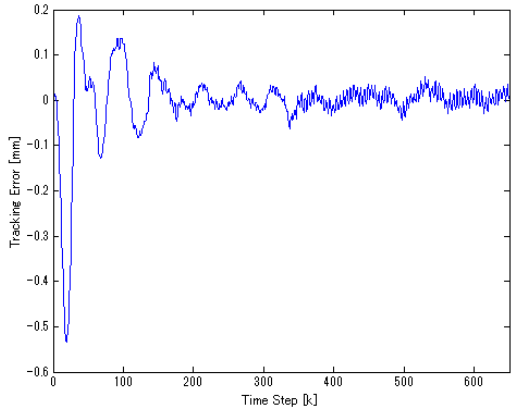

FIGURE 14. Tracking error for $y_{d2}(k)$ with $f = 0.6$.

V. CONCLUSIONS

This paper has addressed the modeling and adaptive control problems for the IPMC actuators. Firstly, a new model, which is expressed by a linear system preceded by Prandtl-Ishlinskii operator, in discrete-time domain is proposed. Then, based on this model, a discrete-time adaptive control law is synthesized for IPMC actuators. The discrete-time adaptive controller guarantees the overall stability of the controlled system, and the position tracking error is controlled by the design parameters. Experimental results have verified the effectiveness of the proposed model and control law.

REFERENCES

[1] K. J. Astrom and B. Wittenmark, *Adaptive Control*. Reading, MA, USA: Addison-Wesley, 1989.

[2] Y. Bar-Cohen, "Turning heads," *IEEE Spectr.*, vol. 41, no. 6, pp. 28–33, Jun. 2004.

[3] M. Brokate and J. Sprekels, *Hysteresis and Phase Transitions*. New York, NY, USA: Springer-Verlag, 1996.

[4] R. Caponetto, S. Graziani, F. Pappalardo, and F. Sapuppo, "Identification of IPMC nonlinear model via single and multi-objective optimization algorithms," *ISA Trans.*, vol. 53, no. 2, pp. 481–488, Mar. 2014.

[5] X. Chen and T. Hisayama, "Adaptive sliding-mode position control for piezo-actuated stage," *IEEE Trans. Ind. Electron.*, vol. 55, no. 11, pp. 3927–3934, Nov. 2008.

[6] X. Chen, "Adaptive sliding mode control for discrete-time multi-input multi-output systems," *Automatica*, vol. 42, no. 3, pp. 427–435, 2006.

[7] Z. Chen and X. Tan, "A control-oriented and physics-based model for ionic polymer–metal composite actuators," *ASME/IEEE Trans. Mechatronics*, vol. 13, no. 5, pp. 519–529, Oct. 2008.

[8] P. J. C. Branco, B. Lopes, and J. A. Dente, "Nonuniformly charged ionic polymer–metal composite actuators: Electromechanical modeling and experimental validation," *IEEE Trans. Ind. Electron.*, vol. 59, no. 2, pp. 1105–1113, Feb. 2012.

[9] G. C. Goodwin and K. S. Sin, *Adaptive Filtering, Prediction and Control*. Englewood Cliffs, NJ, USA: Prentice-Hall, 1984.

[10] G.-Y. Gu, L.-M. Zhu, and C.-Y. Su, "Modeling and compensation of asymmetric hysteresis nonlinearity for piezoceramic actuators with a modified Prandtl–Ishlinskii model," *IEEE Trans. Ind. Electron.*, vol. 61, no. 3, pp. 1583–1595, Mar. 2014.

[11] M. A. Krasnosel'Skii and A. V. Pokrovskii, *Systems With Hysteresis*. New York, NY, USA: Springer-Verlag, 1989.

[12] P. Krejci and K. Kuhnen, "Inverse control of systems with hysteresis and creep," *Proc. Inst. Elect. Eng. Control Theory Appl.*, vol. 148, no. 3, pp. 185–192, 2001.

[13] A. J. McDaid, K. C. Aw, E. Haemmerle, and S. Q. Xie, "A conclusive scalable model for the complete actuation response for IPMC transducers," *Smart Mater. Struct.*, vol. 19, no. 7, p. 075011, 2010.

[14] I. D. Mayergoyz, *Mathematical Models of Hysteresis*. New York, NY, USA: Springer-Verlag, 1991.

[15] S. Nemat-Nasser and J. Li, "Electromechanical response of ionic polymer-metal composites," *J. Appl. Phys.*, vol. 87, no. 7, pp. 3321–3331, 2000.

[16] D. Pugal, P. Solin, A. Aabloo, and K. J. Kim, "IPMC mechanoelectrical transduction: Its scalability and optimization," *Smart Mater. Struct.*, vol. 22, no. 12, p. 125029, 2013.

[17] M. Shahinpoor and K. J. Kim, "Ionic polymer-metal composites: I. Fundamentals," *Smart Mater. Struct.*, vol. 10, no. 4, pp. 819–833, 1991.

[18] C.-Y. Su, Q. Wang, X. Chen, and S. Rakheja, "Adaptive variable structure control of a class of nonlinear systems with unknown Prandtl–Ishlinskii hysteresis," *IEEE Trans. Autom. Control*, vol. 50, no. 12, pp. 2069–2074, Dec. 2005.

[19] X. Tan and J. S. Baras, "Modeling and control of hysteresis in magnetostrictive actuators," *Automatica*, vol. 40, no. 9, pp. 1469–1480, 2004.

[20] G. Tao and P. V. Kokotovic, "Adaptive control of plants with unknown hystereses," *IEEE Trans. Autom. Control*, vol. 40, no. 2, pp. 200–212, Feb. 1995.

[21] A. Visintin, *Differential Models of Hysteresis*. New York, NY, USA: Springer-Verlag, 1994.

XINKAI CHEN (M'95–SM'02) received the Doctoral degree in engineering from Nagoya University, Japan, in 1999. He is currently a Professor with the Department of Electronic Information Systems, Shibaura Institute of Technology, Japan. His research interests include smart materials, hysteresis, adaptive control, and sliding mode control. He served as an Associate Editor for several journals including the IEEE Transactions on Automatic Control, the IEEE Transactions on Control Systems Technology, the IEEE/ASME Transactions on Mechatronics, the IEEE Transactions on Industrial Electronics, and the *European Journal of Control*. He also served for international conferences as an organizing committee member including the program chair and the program co-chair.'